Structural, Elastic, and Electronic Properties of Superhard Monoclinic C_{32} under High Pressure

Xinchao Yang[a], Qun Wei[a,*], Bing Wei[a], Haiyan Yan[b], Ruike Yang[a], Meiguang Zhang[c], Qinghua Chen[d], Xinming Wang[a], Ronghui Yao[a], Chenyang Zhao[e] and Chunying Ding[a]

[a]School of Physics and Optoelectronic Engineering, Xidian University, Xi'an 710071, PR China
[b]Department of Chemistry and Chemical Engineering, Baoji University of Arts and Sciences, Baoji 721013, PR China
[c]College of Physics and Optoelectronic Technology, Nonlinear Research Institute, Baoji University of Arts and Sciences, Baoji 721016, PR China
[d]School of Systems Science, Beijing Normal University, Beijing 100875, PR China
[e]School of Microelectronics, Xidian University, Xi'an 710071, PR China

(Received June 11, 2019; revised version August 25, 2019; in final form September 3, 2019)

The properties of a recently proposed carbon allotrope of monoclinic C_{32}, which is named $C2/m$-32 carbon, were studied by first-principles calculations. This new carbon allotrope has an all-sp^3 hybridized bonding network. The dynamic and mechanical stabilities at 0 GPa and 100 GPa are demonstrated by phonon dispersion and elastic constants, respectively. Studies of the elastic anisotropy of $C2/m$-32 carbon show that the elastic anisotropy increases with the augment of pressure. Surprisingly, the Vickers hardness of this new carbon allotrope is 90.9 GPa, which is almost as hard as diamond. The analysis of electronic band structure shows that $C2/m$-32 carbon is an indirect band gap semiconductor with a band gap of 4.18 eV. These results broaden our understanding of the structural and electronic properties of carbon allotropes.

DOI: 10.12693/APhysPolA.136.940

PACS/topics: first-principles calculations, elastic anisotropy, electronic properties, superhard materials

1. Introduction

Carbon can form a vast variety of allotropes and organic compounds due to its different hybridizations, yielding allotropes such as graphite, diamond, lonsdaleite, carbine, chaoite, fullerenes, nanotubes, graphene, etc. In recent years, the synthesis of new carbon isomers has attracted much attentions. Among them, graphite [1], fullerenes [2], and carbon nanotubes [3] have been explored in experiments, which have had a great impact on the field of materials and information science. Because of its unique properties, diamond stands out as the hardest material among the superhard materials used in industrial operations related to cutting, drilling, turning, grinding, and boring. In the field of synthesizing and predicting new carbon allotropes, superhard carbon allotropes have attracted special attention. Besides these familiar carbon allotropes, other carbon materials have also been investigated. Researchers have obtained many significant achievements [4–14]. Many researchers have studied superhard carbon allotropes, such as the monoclinic phase (M-carbon [15], $C2/m$-20 carbon [16]), the orthorhombic phase (oC$_{20}$ [4], oC$_{32}$ [17]), and the tetragonal C$_{64}$ [18], etc. Experimentally, by compressing graphite at room temperature, M-carbon can be obtained with a decrease in grain size [5, 19], which is more energetically favorable than graphite at pressures higher than 13.4 GPa. Its hardness is 79.2 GPa. The bulk modulus is 404 GPa, which is slightly less than that of diamond. In addition, $C2/m$-32 carbon possesses high bulk modulus of 412 GPa and hardness of 80.1 GPa. Recently, Deringer et al. [20] predicted a new C$_{32}$ phase (named $C2/m$-32) with space group of $C2/m$. The detailed properties of this C$_{32}$ phase have not been studied, hitherto. In the present paper, the structural, mechanical, elastic, and electronic properties of this new $C2/m$-32 phase are studied in detail.

2. Computational details

For the $C2/m$-32 carbon phase, its optimization and dynamic characteristics are calculated by density functional theory (DFT) [21] in the case of generalized gradient approximation (GGA) [22], in the Cambridge series total energy package (CASTEP) [23] code. The electronic properties and optical properties of the structure were analyzed by using the ultrasoft pseudopotential [24], which describes the interaction between ionic core and valence electrons. The Monkhorst-Pack mesh scheme [25] was used to optimize the k-mesh in the first irreducible Brillouin region ($3 \times 19 \times 11$) with a cut-off energy of 600 eV. The Bryden–Fletcher–Goldfarb–Shanno (BFGS) minimization scheme [26] was

*corresponding author; e-mail: weiaqun@163.com

adopted to optimize the structure. The approximation of the computational structure in the generalized gradient is parametrized by Perdew, Burke, and Ernzerhof (PBE). The independent elastic constants were determined from evaluation of stress tensor generated small strain and bulk modulus, shear modulus, Young's modulus, and Poisson's ratio were thus estimated by the Voigt–Reuss–Hill approximation [27]. The convergence value used in all convergence experiments was within 1 meV/atom.

3. Results and discussion

$C2/m$-32 carbon atoms per unit cell have a monoclinic symmetry. The optimized lattice parameters of $C2/m$-32 carbon are a = 17.858 Å, b = 2.526 Å, c = 4.258 Å, β = 103.4°, respectively. In a unit cell, there are eight inequivalent carbon atoms that occupy the Wyckoff 4i sites: C1 (0.6406, 0, 0.4754), C2 (0.7339, 0, 0.5657), C3 (0.7636, 0, 0.9288), C4 (0.6165, 0, 0.1059), C5 (0.8498, 0, 0.0127), C6 (0.5301, 0, 0.8923), C7 (0.6150, 0.5, 0.6282), and C8 (0.5297, 0.5, 0.6669) at GGA level.

Figure 1a shows the full perspective of $C2/m$-32 carbon, where all the atoms are four-coordinated, and nine types of carbocycles are shown in Fig. 1b–d.

As shown in Fig. 1b, there are three types of carbon rings. The C5 ring, which is filled with purple, has five types of atoms (one C4, one C5, one C6, one C7, and one C8), and the bond lengths of C5 ring are 1.535 Å (C4–C5), 1.599 Å (C4–C6), 1.512 Å (C5–C7), 1.585 Å (C6–C8), and 1.568 Å (C7–C8), respectively. The C7 ring is filled with navy blue, and has one C1, one C4, one C7, two C6, and two C8 atoms, and the lengths of C1–C4, C1–C7, C4–C6, C6–C6, C6–C8, C7–C8, and C8–C8 are 1.532 Å, 1.539 Å 1.599 Å, 1.566 Å, 1.585 Å, 1.568 Å, and 1.564 Å, respectively. The C10 ring with the color of green has six types of atoms, one C1, one C4, one C7, two C2, two C5, and three C3 atoms, and the lengths of C1–C4, C1–C7, C2–C2, C2–C3, C3–C3, C3–C5, C4–C5, and C5–C7 are 1.532 Å, 1.539 Å, 1.545 Å, 1.513 Å, 1.528 Å, 1.497 Å, 1.535 Å, and 1.512 Å, respectively.

The C6 ring shown in Fig. 1c has two types. The one with the color of turquoise has three C2 and three C3 atoms, and the lengths of the C6 ring are 1.545 Å (C2–C2), 1.513 Å (C2–C3), and 1.528 Å (C3–C3), respectively. The other one that is filled with red has one C1, one C4, two C5, and two C7 atoms, and the bond lengths of the C6 ring are 1.539 Å (C1–C7), 1.535 Å (C4–C5), and 1.512 Å (C5–C7), respectively.

There are three types of C6 rings and one type of C8 rings shown in Fig. 1d. The three C6 rings are different from the two C6 carbon rings above. One C6 ring is dyed aqua green, and has one C4, two C5, and three C3 atoms, and the lengths are 1.528 Å (C3–C3), 1.497 Å (C3–C5), and 1.535 Å (C4–C5), respectively. Another C6 ring that is filled with yellow has one C1, one C6, two C7, and two C8 atoms, and the bond lengths are 1.539 Å (C1–C7), 1.585 Å (C6–C8), and 1.568 Å (C7–C8), respectively. The third C6 which is filled with light green has three types of bonds, and the lengths are 1.535 Å (C4–C5), 1.599 Å (C4–C6), and 1.585 Å (C6–C8), respectively. The zigzag C8 ring is shown in green. It has one C5, one C8, two C4, and four C6 atoms, and the bond lengths are 1.535 Å (C4–C5), 1.599 Å (C4–C6), 1.566 Å (C6–C6), and 1.585 Å (C6–C8), respectively. The mechanical stability is determined by the elastic properties of a material.

Therefore, for the $C2/m$-32 structure of monoclinic crystal, 13 independent elastic constants (C_{11}, C_{22}, C_{33}, C_{44}, C_{55}, C_{66}, C_{12}, C_{13}, C_{15}, C_{23}, C_{25}, C_{35}, and C_{46}) were calculated and listed in Table I.

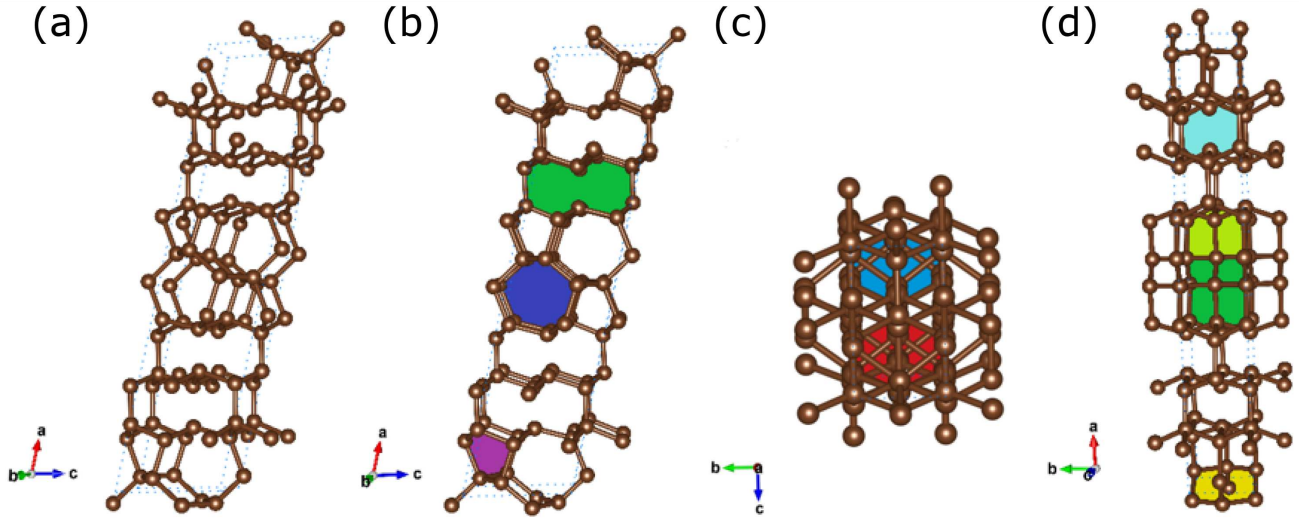

Fig. 1. (a) Full perspective of the $C2/m$-32 carbon in a conventional cell, (b) the structure of $C2/m$-32 carbon observed from the direction of [010], (c) the structure of $C2/m$-32 carbon observed from the direction of [100], (d) the structure of $C2/m$-32 carbon observed from the direction of [001]. All the carbon atoms are nut-brown.

TABLE I

Calculated elastic constants C_{ij} [GPa], bulk modulus B [GPa], shear modulus G [GPa], Young's modulus E [GPa], Poisson's ratio ν, B/G ratio, and the hardness H [GPa] of the $C2/m$-32 carbon, diamond, oC$_{20}$, c-BN, M-carbon, and C$_{64}$.

	Diamond	$C2/m$-32[a]		M-carbon	oC$_{20}$	c-BN	C$_{64}$
Pressure [GPa]	0	0	100	0	0	0	0
C_{11}	1053[b]	1114	1664	929[c]	794[d]	779[e]	598[f]
C_{22}		1117	1732	1087[c]	760[d]		
C_{33}		1149	1723	1044[c]	979[d]		677[f]
C_{44}	563[b]	535	715	929[c]	794[d]	779[e]	598[f]
C_{55}		480	636	452[c]	251[d]		
C_{66}		446	546	389[c]	261[d]		107[f]
C_{12}	120[b]	49	206	49[c]	112[d]	165[e]	43[f]
C_{13}		64	288	156[c]	61[d]		108[f]
C_{15}		20	37	63[c]			
C_{23}		84	318	87[c]	75[d]		
C_{25}		−44	−100	−28[c]			
C_{35}		39	84	26[c]			
C_{46}		−37	−80	−8[c]			
B	431[b]	419	749	404[c]	335[d]	370[e]	264[f]
G	522[b]	502	657	454[c]	327[d]	384[e]	217[f]
E	1116[b]	1076	1525	991[c]	742[d]	856[e]	510[f]
ν	0.07[b]	0.07	0.16	0.09[c]	0.13$_d$	0.12[e]	0.18[f]
B/G		0.83	1.14		1.02[d]		1.22[f]
$H_{(Chen--Niu)}$	94.3[a]	90.9	73.3	79.2[a]	54.5[a]	64.9[a]	34.0[a]
$H_{(Lyakhov--Oganov)}$	96.0[a]	92.3	78.3	79.9[a]	54.0[a]	54.8[a]	36.1[a]

[a] this work, [b] Ref. [28], [c] Ref. [29], [d] Ref. [4], [e] Ref. [30], [f] Ref. [18]

The elastic constants of a crystal with monoclinic symmetry should obey the following generalized Born mechanical stability criterion at 0 GPa [31, 32]:

$$C_{ii} > 0, \quad i = 1, \ldots, 6, \tag{1}$$

$$C_{11} + C_{22} + C_{33} + 2\,(C_{12} + C_{13} + C_{23}) > 0, \tag{2}$$

$$C_{33}C_{55} - C_{35}^2 > 0, \tag{3}$$

$$C_{44}C_{66} - C_{46}^2 > 0, \tag{4}$$

$$C_{22} + C_{33} - 2C_{23} > 0, \tag{5}$$

$$C_{22}\left(C_{33}C_{55} - C_{35}^2\right) + 2C_{23}C_{25}C_{35} - C_{23}^2C_{55} - C_{25}^2C_{33} > 0, \tag{6}$$

$$2\big[C_{15}C_{25}\left(C_{33}C_{12} - C_{13}C_{23}\right) + C_{15}C_{35}\left(C_{22}C_{13} - C_{12}C_{33}\right) + C_{25}C_{35}\left(C_{11}C_{23} - C_{12}C_{13}\right)\big] - \big[C_{15}^2\left(C_{22}C_{33} - C_{23}^2\right) + C_{25}^2\left(C_{12}C_{33} - C_{13}^2\right) + C_{35}^2\left(C_{12}C_{22} - C_{12}^2\right)\big] + gC_{55} > 0, \tag{7}$$

$$g = C_{11}C_{22}C_{33} - C_{11}C_{23}^2 - C_{22}C_{13}^2 - C_{33}C_{12}^2 + 2\,C_{12}C_{13}C_{23}. \tag{8}$$

The mechanical stability in crystals at high pressures is provided by [33, 34]. This requires that the symmetric matrix

$$\hat{G} = \begin{bmatrix} \tilde{C}_{11} & \tilde{C}_{12} & \tilde{C}_{13} & 2C_{14} & 2C_{15} & 2C_{16} \\ \tilde{C}_{21} & \tilde{C}_{22} & \tilde{C}_{23} & 2C_{24} & 2C_{25} & 2C_{26} \\ \tilde{C}_{31} & \tilde{C}_{32} & \tilde{C}_{33} & 2C_{34} & 2C_{35} & 2C_{36} \\ 2C_{41} & 2C_{42} & 2C_{43} & 4C_{44} & 4C_{45} & 4C_{46} \\ 2C_{51} & 2C_{52} & 2C_{53} & 4C_{54} & 4C_{55} & 4C_{56} \\ 2C_{61} & 2C_{62} & 2C_{63} & 4C_{64} & 4C_{65} & 4C_{66} \end{bmatrix} \tag{9}$$

should have a positive determinant. In Eq. (9):

$$\tilde{C}_{\alpha\alpha} = C_{\alpha\alpha} - P, \quad \alpha = 1, \ldots, 6, \tag{10}$$

$$\tilde{C}_{12} = C_{12} + P, \quad \tilde{C}_{13} = C_{13} + P, \quad \tilde{C}_{23} = C_{23} + P, \tag{11}$$

where P is the isotropic pressure.

As can be seen from Table I, the calculated results of the $C2/m$-32 phase satisfy the criteria at 0 and 100 GPa, showing a mechanical stability. In addition, we calculated the phonon spectra of $C2/m$-32 carbon at 0 GPa and 100 GPa to determine the dynamical stability. As can be seen from Fig. 2, there is no negative frequency in the whole Brillouin region, which indicates that the structure is dynamically stable at least up to 100 GPa.

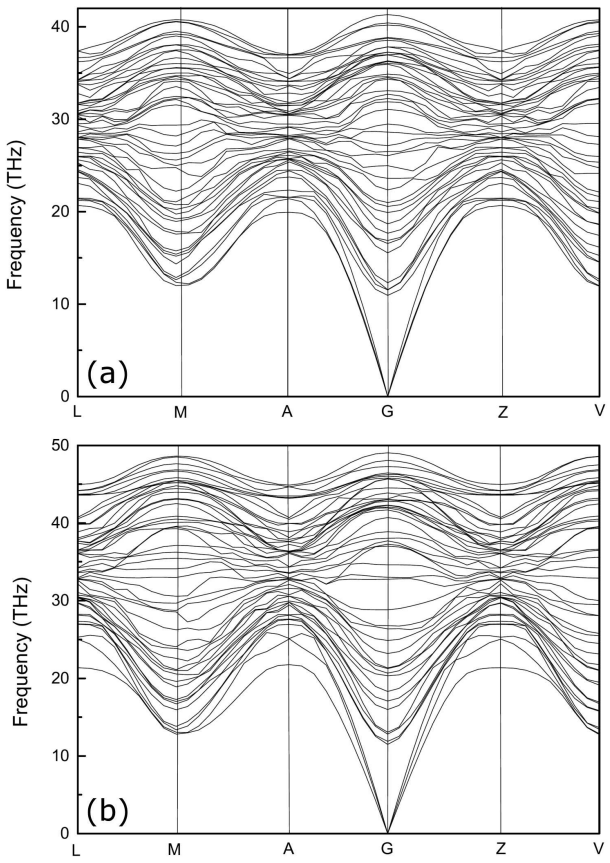

Fig. 2. The phonon spectra of $C2/m$-32 carbon under 0 GPa (a) and 100 GPa (b).

From Table I, one can see that the C_{11} values of oC$_{20}$ (794 GPa), c-BN (779 GPa), M-carbon (929 GPa), and C$_{64}$ (598 GPa) are less than that of $C2/m$-32 carbon (1114 GPa), which is even larger than that of diamond (1053 GPa). The larger C_{11}, C_{22}, and C_{33} values of $C2/m$-32 carbon indicate that $C2/m$-32 carbon have stronger compression resistance along the a-, b-, and c-axes, respectively.

In order to understand the elastic properties of $C2/m$-32 phase, we calculated elastic constants under pressure and illustrated in Fig. 3. As seen from Fig. 3, with the increase of pressure, all elastic constants show an increasing trend, and C_{11}, C_{22}, and C_{33} grow faster than other elastic constants, except that the values of C_{25} and C_{46} show a decreasing trend. The bulk modulus B and shear modulus G of the crystal at various pressures were calculated using the Voigt–Reuss–Hill approximation, and the results of other allotropes are also listed for comparison in Table I. Both the bulk modulus B and shear modulus G of $C2/m$-32 carbon are larger than those of M-carbon, c-BN, oC$_{20}$, and C$_{64}$, respectively, and are close to those of diamond, indicating that $C2/m$-32 carbon has a strong ability to resist compression deformation of materials. According to Pugh, we know that the ratio of B to G can reflect

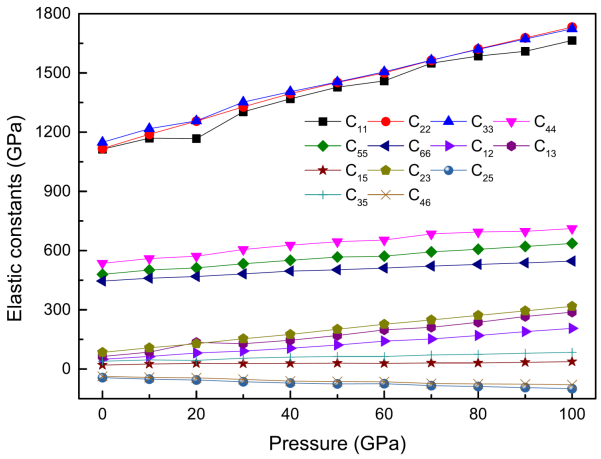

Fig. 3. The elastic constants of $C2/m$-32 carbon as a function of pressure.

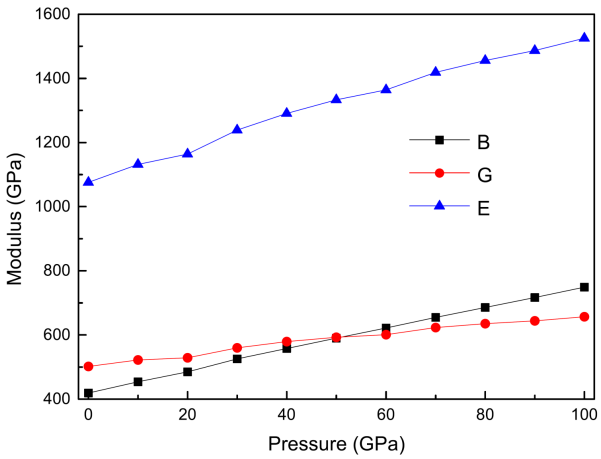

Fig. 4. Elastic modulus of $C2/m$-32 carbon as a function of pressure.

the brittleness and ductility of materials. If the value of B/G is less than 1.75, the material shows brittleness; otherwise, it shows ductility [33, 35]. The ratio for $C2/m$-32 carbon is 0.83, indicating its brittleness nature. The Young modulus E and the Poisson ratio ν are given by the following equations [27, 36]:

$$E = \frac{9BG}{3B+G}, \tag{12}$$

$$\nu = \frac{3B-2G}{2(3B+G)}. \tag{13}$$

The two parameters above are identified to be related with hardness. The Young modulus E of $C2/m$-32 carbon is 1076 GPa. The value of Young's modulus indicates the rigidity of the material. The larger Young modulus is, the less likely it is to be deformed. As is well known, diamond is one of the stiffest materials due to its large value of E. The Poisson ratio ν of $C2/m$-32 carbon is known as 0.07 from Table I.

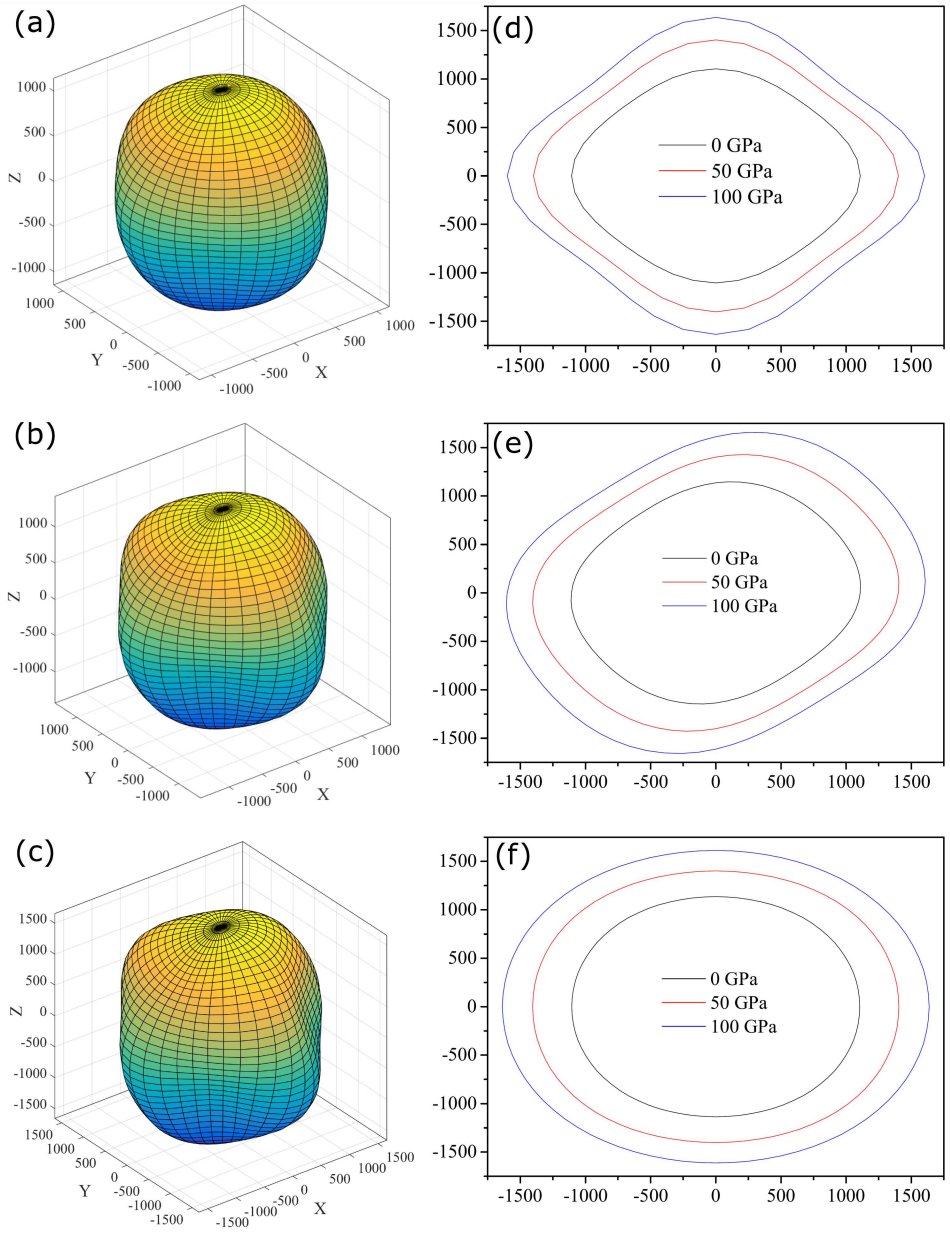

Fig. 5. Three-dimensional surface representations of the Young modulus for the $C2/m$-32 carbon at 0 GPa (a), 50 GPa (b), and 100 GPa (c), respectively, and the projections of the directional dependent Young modulus in different planes: xy plane (d), xz plane (e), and yz plane (f).

To further understand the mechanical properties, the values of volume modulus B, shear modulus G, and Young's modulus E under different pressures were illustrated as shown in Fig. 4. From Fig. 4, one can see that each modulus tends to increase with pressures, and the bulk modulus increases faster than the shear modulus. The hardness of $C2/m$-32 calculated by is 90.9 GPa (by Chen–Niu model [37]) $\sim$ 92.3 GPa (by Lyakhov–Oganov model [13]), which indicates that $C2/m$-32 carbon is a potential superhard material. The elastic anisotropy of materials has an important impact on their physical and mechanical properties. Therefore, based on the fundamental elastic constants, the elastic anisotropy can be shown by a three-dimensional figure. For a monoclinic system, the directional dependence of Young's modulus E can be written as [38]:

$$E^{-1} = l_1^4 S_{11} + 2l_1^2 l_2^2 S_{12} + 2l_1^2 l_3^2 S_{13} + 2l_1^3 l_3 S_{15} + l_2^4 S_{22}$$

$$+2l_2^2 l_3^2 S_{23} + 2l_1 l_2^2 l_3 S_{25} + l_3^4 S_{33} + 2l_1^3 S_{35} + l_2^2 l_3^2 S_{44}$$

$$+2l_1 l_2^2 l_3 S_{46} + l_1^2 l_3^2 S_{55} + l_1^2 l_2^2 S_{66}, \qquad (14)$$

where l_1, l_2, and l_3 are the direction cosines, and S_{ij} are the elastic compliance constants.

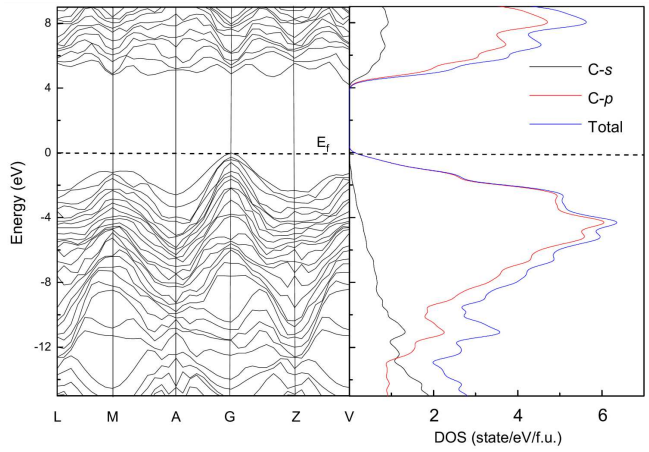

Fig. 6. Electronic band structure and density of states for the $C2/m$-32 carbon at 0 GPa within GGA.

For the $C2/m$-32 carbon, the three-dimensional diagram of Young's modulus at various pressures are given in Fig. 5a–c. For isotropic systems, the three-dimensional diagram is spherical, whereas for anisotropic systems, the three-dimensional graph is ellipsoidal. In other words, the degree of spherical deviation reflects the size of the anisotropy [39]. From Fig. 5a–c, we found that the three-dimensional diagram of Young's modulus of $C2/m$-32 carbon under various pressures is ellipsoidal and shows its anisotropy. Under 0 GPa, 50 GPa, and 100 GPa, the maximum values of E are 1164 GPa, 1468 GPa and 1715 GPa, respectively, and the minimum values are 978 GPa, 1154 GPa, and 1283 GPa, respectively. Meanwhile, the mean value of Young's modulus at 0 GPa is 1089 GPa, which is basically consistent with the approximate value calculated by the Voigt–Reuss–Hill approximations (1076 GPa). For $C2/m$-32 carbon, the $E_{\max}/E_{\min}$ ratios are 1.19, 1.27, and 1.33, respectively. The ratio of Young's modulus increases with pressure, and the anisotropy becomes more obvious.

The projections of the directionally dependent Young's modulus in different planes: xy plane, xz plane, and yz plane are shown in Fig. 5d–f. It can be seen that the anisotropy of Young's modulus of each plane increases with the increase of pressure. The universal anisotropic index A^U was evaluated by [40]:

$$A^U = 5\frac{G_V}{G_R} + \frac{B_V}{B_R} - 6, \tag{15}$$

where the subscripts V and R represent the Voigt and Reuss approximation of the bulk and shear modulus, respectively. As A^U goes to 0, the more isotropic the crystal becomes. On the contrary, the anisotropy is more obvious. At 0 GPa, 50 GPa, and 100 GPa, the values of the universal anisotropic index A^U of $C2/m$-32 carbon are 0.05, 0.10, and 0.14, respectively. This means that the elastic anisotropy increases with pressure, which conforms to the change of the trend of ratio of Young's modulus.

The band structure and density of state (DOS) of $C2/m$-32 carbon under 0 GPa are calculated and shown in Fig. 6. One can see that the band structure of $C2/m$-32 carbon changes in the corresponding Brillouin region path and the contribution of electrons in the corresponding orbitals. The band gap of $C2/m$-32 carbon is 4.18 eV, which is slightly larger than that of diamond (4.16 eV) [41]. In general, the actual band gap calculated by DFT usually underestimated about 30% to 50%, so the actual energy difference will be larger [30]. For $C2/m$-32 carbon, the conduction band minimum (CBM) is located at the V point and the valence band maximum (VBM) is located at the G point. In addition, for valence band and conduction band, the main contribution of DOS near Fermi energy level comes from C-p orbital electrons, while C-s contributes less to total DOS.

4. Conclusions

In a word, a new structure of $C2/m$-32 carbon has been studied. By using the first-principles calculation, we demonstrated that the structure is mechanical and dynamical at ambient pressure. It has nine types of carbon rings, including one C5, one C7, one C8, one C10, and five C6 carbon rings. The elastic constants, modulus of elasticity, Poisson's ratio, and phonon spectrum are calculated by the above method. The directional dependence of Young's modulus at various pressures in different plains shows the elastic anisotropy of the $C2/m$-32 carbon. The Vickers hardness calculated by Chen–Niu model is 90.9 GPa. The $C2/m$-32 carbon structure is a semiconductor material with an indirect band gap of 4.18 eV. The detailed analyses of the structure under various pressures reveal that the $C2/m$-32 carbon is a potential superhard material.

Acknowledgments

This work was financially supported by the Natural Science Foundation of China (Grant No. 11965005 and 11964026), the Natural Science New Star of Science and Technologies Research Plan in Shaanxi Province of China (Grant No. 2017KJXX-53), the 111 Project (B17035), and Natural Science Basic Research plan in Shaanxi Province of China (Grant No. 2019JM-353). Xiao-Feng Shi is acknowledged for comments on the manuscript. All the authors thank the computing facilities at High Performance Computing Center of Xidian University.

References

[1] K.S. Novoselov, A.K. Geim, S.V. Morozov, D. Jiang, Y. Zhang, S.V. Dubonos, I.V. Grigorieva, A.A. Firsov, *Science* **306**, 666 (2004).

[2] H.W. Kroto, J.R. Heath, S.C. O'Brien, R.F. Curl, R.E. Smaliey, *Nature* **318**, 162 (1985).

[3] S. Iijima, *Nature* **354**, 56 (1991).

[4] Q. Wei, C.Y. Zhao, M.G. Zhang, H.Y. Yan, Y.J. Zhou, R.H. Yao, *Phys. Lett. A* **382**, 1685 (2018).

[5] S.E. Boulfelfel, A.R. Oganov, S. Leoni, *Sci. Rep.* **2**, 00471 (2012).

[6] C. Piskoti, J. Yarger, A. Zettl, *Nature* **393**, 771 (1998).

[7] D. Li, F.B. Tian, B.H. Chu, D.F. Duan, X.J. Sha, Y.Z. Lv, H.D. Zhang, N. Lu, B.B. Liu, T. Cui, *Sci. Rep.* **5**, 13447 (2015).

[8] W.L. Mao, H.K. Mao, P.J. Eng, T.P. Trainor, M. Newville, C.-C. Kao, D.L. Heinz, J.F. Shu, Y. Meng, R.J. Hemley, *Science* **302**, 425 (2003).

[9] M. Hu, Z.S. Zhao, F. Tian, A.R. Oganov, Q.Q. Wang, M. Xiong, C.Z. Fan, B. Wen, J.L. He, D.L. Yu, H.-T. Wang, B. Xu, Y.J. Tian, *Sci. Rep.* **3**, 1331 (2013).

[10] M. Amsler, J.A. Flores-Livas, M.A.L. Marques, S. Botti, S. Goedecker, *Eur. Phys. J. B* **86**, 383 (2013).

[11] S. Yamanaka, A. Kubo, K. Inumaru, K. Komaguchi, N.S. Kini, T. Inoue, T. Irifune, *Phys. Rev. Lett.* **96**, 076602 (2006).

[12] Q. Huang, D.L. Yu, B. Xu, W.T. Hu, Y.M. Ma, Y.B. Wang, Z.S. Zhao, B. Wen, J.L. He, Z.Y. Liu, Yongjun Tian, *Nature* **510**, 250 (2014).

[13] A.O. Lyakhov, A.R. Oganov, *Phys. Rev. B* **84**, 092103 (2011).

[14] A. Pokropivny, S. Volz, *Phys. Status Solidi B* **249**, 1704 (2012).

[15] Q. Li, Y.M. Ma, A.R. Oganov, H.B. Wang, H. Wang, Y. Xu, T. Cui, H.-K. Mao, G.T. Zou, *Phys. Rev. Lett.* **102**, 175506 (2009).

[16] M.J. Xing, B.H. Li, Z.T. Yu, Q. Chen, *RSC Adv.* **6**, 32740 (2016).

[17] M. Zhang, H.Y. Liu, Y.H. Du, X.X. Zhang, Y.C. Wang, Q. Li, *Phys. Chem. Chem. Phys.* **15**, 14120 (2013).

[18] Q. Wei, Q. Zhang, H.Y. Yan, M.G. Zhang, *J. Mater. Sci.* **52**, 2385 (2017).

[19] Y.J. Wang, J.E. Panzik, B. Kiefer, K.K.M. Lee, *Sci. Rep.* **2**, 00520 (2012).

[20] V.L. Deringer, G. Csanyi, D.M. Proserpio, *Chem. Phys. Chem.* **18**, 873 (2017).

[21] W. Kohn, L.J. Sham, *Phys. Rev.* **140**, A1133 (1965).

[22] J.P. Perdew, K. Burke, M. Ernzerhof, *Phys. Rev. Lett.* **77**, 3865 (1996).

[23] S.J. Clark, M.D. Segall, C.J. Pickard, P.J. Hasnip, M.I.J. Probert, K. Refson, M.C. Payne, *Z. Kristallogr.* **220**, 567 (2005).

[24] D. Vanderbilt, *Phys. Rev. B* **41**, 7892 (1990).

[25] H.J. Monkhorst, J.D. Pack, *Phys. Rev. B* **13**, 5188 (1976).

[26] B.G. Pfrommer, M. Côté, S.G. Louie, M.L. Cohen, *J. Comput. Phys.* **131**, 233 (1977).

[27] R. Hill, *Phys. Soc. A* **65**, 349 (1952).

[28] Q.Y. Fan, Q. Wei, C.C. Chai, H.Y. Yan, M.G. Zhang, Z.Z. Lin, Z.X. Zhang, J.Q. Zhang, D.Y. Zhang, *J. Phys. Chem. Solids* **79**, 89 (2015).

[29] Z.P. Li, F.M. Gao, Z.M. Xu, *Phys. Rev. B* **85**, 144115 (2012).

[30] Q.Y. Fan, Q. Wei, C.C. Chai, M.G. Zhang, H.Y. Yan, Z.X. Zhang, J.Q. Zhang, D.Y. Zhang, *Comput. Mater. Sci.* **97**, 6 (2015).

[31] Q.Y. Fan, Q. Wei, H.Y. Yan, M.G. Zhang, D.Y. Zhang, J.Q. Zhang, *Acta Phys. Pol. A* **126**, 740 (2014).

[32] Z.J. Wu, E.J. Zhao, H.P. Xiang, X.F. Hao, X.J. Liu, Jian Meng, *Phys. Rev. B* **76**, 054115 (2007).

[33] Q. Wei, Q. Zhang, M.G. Zhang, *Materials* **9**, 570 (2016).

[34] G.V. Sin'ko, N.A. Smirnov, *J. Phys. Condens. Matter* **14**, 6989 (2002).

[35] S.F. Pugh, *Philos. Mag.* **45**, 823 (1954).

[36] Q. Wei, C. Zhao, M. Zhang, H. Yan, B. Wei, *Phys. Lett. A* **383**, 2429 (2019).

[37] X.Q. Chen, H.Y. Niu, D.Z. Li, Y.Y. Li, *Intermetallics* **19**, 1275 (2011).

[38] S. Qiu, B. Clausen, S.A. Padula II, R.D. Noebe, R. Vaidyanathan, *Acta Mater.* **59**, 5055 (2011).

[39] W.C. Hu, Y. Liu, D.J. Li, X.Q. Zeng, C.S. Xu, *Comput. Mater. Sci.* **83**, 27 (2014).

[40] S.I. Ranganathan, M. Ostoja-Starzewski, *Phys. Rev. Lett.* **101**, 055504 (2008).

[41] Q.Y. Fan, Q. Wei, H.Y. Yan, M.G. Zhang, Z.X. Zhang, J.Q. Zhang, D.Y. Zhang, *Comput. Mater. Sci.* **85**, 80 (2014).